MATERIALE PLASTICE
https://revmaterialeplastice.ro
https://doi.org/10.37358/Mat.Plast.1964

Preparation and pH-Responsive Behavior of GO–CS–DOX Nanoparticles: A Preliminary *In Vitro* Evaluation

WEI CAO[1,2,#], QI SHAO[3,#], JUN ZHU[2,4], LI MING[2,4], YANG YANG[5,6*], WEICHANG CHEN[1*]
[1] Department of Gastroenterology, The First Affiliated Hospital of Soochow University, Suzhou, 215006, China
[2] Department of Gastroenterology, Affiliated Hospital of Nantong University, Nantong, 226001, China
[3] Department of Chemotherapy, Affiliated Hospital of Nantong University, Nantong, 226001, China
[4] Department of Chemotherapy, Rugao Hospital, Affiliated Hospital of Nantong University, Rugao, Nantong, 226500, China
[5] Department of Emergency Medicine, Affiliated Hospital of Nantong University, Nantong, 226001, China
[6] Department of Chemistry, School of Science, China Pharmaceutical University, Nanjing, 211198, China

Abstract: ***Background:*** *Gastric cancer remains one of the leading causes of cancer-related deaths worldwide, and the development of effective, targeted drug delivery systems is crucial to improve therapeutic outcomes. Graphene oxide (GO)-based nanocarriers have shown promise for controlled drug release, yet their biological evaluation remains limited.* ***Methods:*** *We synthesized a composite nanoparticle system by electrostatic self-assembly of chitosan (CS) onto graphene oxide (GO), followed by doxorubicin (DOX) loading. The resulting GO–CS–DOX nanoparticles were characterized by transmission electron microscopy (TEM), dynamic light scattering (DLS), zeta potential, and pH-responsive release profiles. Preliminary biological performance was evaluated in gastric cancer cells (AGS), including dose–response cytotoxicity and fluorescence-based uptake studies.* ***Results:*** *GO–CS–DOX nanoparticles showed a clear pH-dependent DOX release behavior, with accelerated release under mildly acidic conditions. DLS and zeta potential measurements confirmed successful drug loading and changes in surface charge. In vitro, GO–CS–DOX demonstrated comparable or slightly enhanced cytotoxicity relative to free DOX at specific concentrations. Cellular uptake of DOX was observed under acidic conditions, consistent with lysosomal trafficking. However, only preliminary in vitro data were collected and no mechanistic apoptosis studies were performed.* ***Conclusion:*** *This study presents the design and initial evaluation of a pH-responsive GO–CS–DOX nanocarrier. While the in vitro results indicate potential for controlled drug release and tumor-targeted delivery, the biological findings are still limited and should be interpreted as preliminary. Further in-depth studies, including apoptosis assays and in vivo validation, are necessary to fully establish therapeutic efficacy.*

Keywords: *Gastric cancer, pH-responsive, graphene oxide, chitosan, doxorubicin, controlled release, nanocarrier*

1. Introduction

Gastric cancer remains one of the leading causes of cancer-related mortality worldwide, largely due to late diagnosis and poor therapeutic response in advanced stages [1,2]. Although doxorubicin (DOX) is a widely used chemotherapeutic agent in gastric cancer treatment, its clinical application is often limited by systemic toxicity, poor tumor selectivity, and rapid clearance [3,4]. To address these challenges, nanocarrier-based drug delivery systems have attracted increasing attention for their ability to improve drug accumulation at tumor sites while minimizing off-target effects [5,6]. Among them, stimuli-responsive nanocarriers, particularly pH-sensitive systems, hold great promise in exploiting the acidic tumor microenvironment to achieve controlled and localized drug release [7–9].

Graphene oxide (GO), a two-dimensional carbon-based nanomaterial, has emerged as a highly suitable platform for drug delivery owing to its large surface area, high drug loading capacity, and

*email: yangyang286228@ntu.edu.cn; cwntvip@163.com
[#] *These authors contributed equally to this work*

ease of surface modification [10–12]. However, pristine GO tends to aggregate under physiological conditions and lacks sufficient biocompatibility for direct biomedical use [13,14]. To overcome these drawbacks, chitosan (CS), a natural cationic polysaccharide with excellent biocompatibility and pH-responsive solubility, can be used to functionalize GO surfaces [15,16]. CS not only improves colloidal stability but also introduces a pH-sensitive shell that dissolves more readily under acidic conditions, thereby enabling pH-triggered drug release [17,18].

In this study, we designed a GO-CS-DOX nanocarrier system that combines the structural advantages of GO with the pH-responsive properties of CS to realize on-demand release of DOX in acidic tumor environments. We systematically characterized the physicochemical properties of the nanoparticles through TEM, DLS, zeta potential, and FTIR analyses. We further investigated their drug loading and encapsulation efficiency under different GO:CS ratios and examined pH-triggered release kinetics and fluorescence behavior. Finally, we conducted preliminary cellular experiments to evaluate the uptake and cytotoxic effects of the nanocarriers in gastric cancer cells. While the *in vitro* data are limited, the results provide initial support for the feasibility of this pH-responsive delivery system and offer a foundation for further optimization and *in vivo* validation.

2. Materials and methods

2.1. Preparation of GO-CS-DOX nanoparticles

Graphene oxide (GO) was synthesized via a modified Hummers' method and dispersed in deionized water under sonication to form a 1 mg/mL stock solution. Chitosan (CS) was dissolved in 1% acetic acid to prepare a 2 mg/mL solution. GO and CS were mixed at various mass ratios (GO:CS = 1:1 to 5:1), stirred for 12 h at room temperature to allow electrostatic self-assembly. Doxorubicin hydrochloride (DOX) was added at a final concentration of 0.2 mg/mL and incubated in the dark for 6 h to load onto GO-CS via π–π stacking and electrostatic interactions. Unbound DOX was removed by centrifugation at 12,000 rpm for 15 min and washed with PBS twice.

2.2. Transmission electron microscopy (TEM) imaging

A drop of the nanoparticle suspension was deposited on a 200-mesh carbon-coated copper grid and dried under vacuum. The samples were imaged using a transmission electron microscope (JEOL, JEM-2100) at an accelerating voltage of 200 kV. Particle size uniformity was qualitatively assessed based on visual distribution.

2.3. Dynamic light scattering (DLS) and zeta potential

The hydrodynamic diameter and polydispersity index (PDI) of the nanoparticles were measured using a Zetasizer Nano ZS (Malvern Instruments) at 25°C, with all samples diluted in PBS to 0.1 mg/mL. Zeta potential was measured using the same instrument, with three replicate readings averaged per sample. GO, CS, and GO-CS-DOX groups were analyzed. To evaluate the surface charge of chitosan, a 0.1% (w/v) aqueous chitosan solution was prepared by dissolving low molecular weight chitosan (degree of deacetylation ~85%) in deionized water and adjusting the pH to 5.5 using 0.1 M HCl. The solution was magnetically stirred overnight at room temperature until fully solubilized and slightly turbid.

2.4. Fourier-transform infrared spectroscopy (FTIR)

Freeze-dried samples of GO and GO-CS-DOX were mixed with KBr powder and pressed into transparent pellets. Spectra were recorded using a Nicolet 6700 FTIR spectrometer in the 4000–400 cm^{-1} range at a resolution of 4 cm^{-1} over 32 scans.

2.5. Loading efficiency and encapsulation efficiency

DOX content in the supernatant after loading was quantified by UV-Vis spectrophotometry at 480 nm. Loading efficiency (%) = (mass of loaded DOX/total nanoparticle mass) × 100%.

Encapsulation efficiency (%) = (mass of loaded DOX/initial DOX added) × 100%. Calibration was performed using a DOX standard curve. Each formulation (GO:CS ratios 1–5) was tested in triplicate.

2.6. *In vitro* drug release

DOX-loaded nanoparticles (2 mg) were suspended in 5 mL of PBS at pH 7.4 or pH 5.5 and placed in dialysis bags (MWCO 3.5 kDa). Bags were incubated in 50 mL PBS at 37°C with gentle shaking. At predetermined time points (0–48 h), 1 mL of release medium was withdrawn and replaced with fresh PBS. DOX concentration was measured by UV-Vis at 480 nm, and cumulative release percentage was calculated.

2.7. Fluorescence spectra

After 48 h of release at pH 7.4 or 5.5, samples were filtered and scanned using a fluorescence spectrophotometer (λ_ex = 480 nm, scan range: 500–700 nm). Spectra were normalized, and fluorescence intensity compared to assess relative DOX release.

2.8. Cell viability assay

Gastric cancer cells (e.g., MKN-45 or AGS) were seeded in 96-well plates at a density of 1×10^4 cells/well and cultured for 24 h. Cells were treated with GO-CS-DOX (DOX equiv. 5 μg/mL) or blank media for 12, 24, and 48 h. After treatment, cell viability was assessed using the CCK-8 assay (Dojindo). 10 μL of CCK-8 solution was added to each well, incubated for 2 h, and absorbance at 450 nm was measured using a microplate reader.

2.9. Cellular uptake analysis

Cells were seeded and treated under the same conditions as in the viability assay. At each time point (12, 24, 48 h), cells were washed with PBS, trypsinized, and resuspended in PBS for flow cytometry. DOX fluorescence (excitation 488 nm, emission collected at 575/26 nm) was quantified using a BD FACSCanto II cytometer. Mean fluorescence intensity (MFI) was calculated from 10,000 gated events per sample. Blank group (no DOX) served as control.

3. Results

To elucidate the pH-triggered release behavior of the nanocarrier system, a schematic diagram was constructed as shown in Figure 1. At pH 7.4, which represents the normal extracellular environment, the chitosan coating effectively encapsulates the GO core and hinders premature leakage of DOX. In contrast, when the pH decreases to 5.5, simulating the acidic microenvironment commonly observed in gastric tumors, the chitosan structure loosens or dissolves, resulting in a burst-like release of DOX [19]. The schematic highlights the structural change of the CS shell and the outward diffusion of DOX, providing visual confirmation of the design rationale behind the pH-sensitive delivery system.

Comprehensive characterization results of the GO-CS-DOX nanocarriers are presented in Figure 2. The TEM image in Figure 2A reveals that the nanoparticles exhibit a relatively broad size distribution, with diameters predominantly under 200 nm. The particles show a quasi-spherical to irregular morphology, suggesting the flexibility of the GO core and the non-uniform coating of chitosan and drug molecules. This level of polydispersity is consistent with many GO-based hybrid nanostructures. Figure 2B shows that GO alone displays a negative surface charge (–30.4 mV) due to abundant surface carboxyl groups. Upon coating with positively charged chitosan, the zeta potential shifts to +42.6 mV, indicating successful electrostatic or hydrogen bonding interactions between CS and GO. Subsequent loading of DOX reduces the surface potential to –12.3 mV, reflecting charge shielding by the neutral or slightly negative DOX molecules and confirming their association with the carrier. The DLS analysis in Figure 2C shows that the average hydrodynamic size increases from ~160 nm for GO to ~210 nm for GO-CS, and further to ~235 nm for GO-CS-DOX, consistent with surface layer formation and drug incorporation. Compared to the TEM image, the slightly larger DLS sizes are attributed to the

hydration shell around nanoparticles in solution. In Figure 2D, the FTIR spectra present a combination of peaks including broad bands near 3400 cm^{-1} (–OH/NH stretching), 1620–1650 cm^{-1} (C=O or N–H bending), and sharp bands corresponding to aromatic or amide groups from DOX. The presence of overlapping and shifted peaks suggests successful integration of all three components—GO, CS, and DOX—into a single nanostructure. Upon DOX loading, the zeta potential of GO-CS nanoparticles shifted from a positive value to approximately −12.3 mV. While DOX·HCl is cationic in nature, this reversal of surface charge is not directly due to the intrinsic charge of DOX, but rather a result of surface adsorption phenomena. Specifically, DOX molecules are known to interact with graphene oxide via π–π stacking, hydrogen bonding, and electrostatic interactions. Once adsorbed onto the GO-CS surface, the DOX molecules can effectively mask or neutralize the surface amino groups of chitosan that originally conferred a positive zeta potential. Furthermore, the adsorption may lead to partial exposure of the underlying GO structure, which carries abundant carboxyl and hydroxyl groups contributing to a net negative surface potential. These combined effects lead to the observed decrease and inversion in zeta potential after DOX loading.

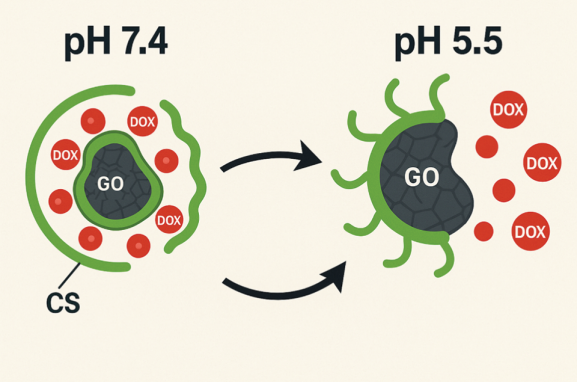

Figure 1. Schematic illustration of the fabrication and pH-responsive drug release mechanism of GO–CS–DOX nanocarriers. Graphene oxide (GO) nanosheets were coated with chitosan (CS) via electrostatic interaction and then loaded with doxorubicin (DOX) through π–π stacking and hydrogen bonding. In neutral physiological environments (pH 7.4), the drug remains stably associated with the carrier due to strong interactions. Under acidic conditions (pH ~5.5), protonation of the amino groups on CS disrupts the interactions with GO and weakens the binding forces with DOX. This facilitates accelerated drug release in acidic tumor microenvironments or endo/lysosomal compartments, enabling pH-triggered therapeutic action

To investigate the formulation optimization and pH-responsiveness of GO-CS-DOX nanocarriers, loading behavior and drug release performance were systematically evaluated, as shown in Figure 3. Figure 3A shows that the loading efficiency gradually increased as the GO:CS ratio increased from 1:1 to 3:1, reaching a peak (~15.8%), and then decreased slightly at higher ratios (4:1 and 5:1). This suggests that an optimal amount of chitosan facilitates drug interaction, while excessive coating may hinder drug access to GO surfaces. Correspondingly, the encapsulation efficiency (Figure 3B) followed a similar trend, with the highest value (~70.1%) at a GO:CS ratio of 3:1. These data indicate that a 3:1 ratio balances efficient drug loading and nanoparticle stability. Figure 3C displays the *in vitro* cumulative release profiles of DOX under neutral (pH 7.4) and acidic (pH 5.5) conditions. Under pH 5.5, the release was markedly accelerated, exceeding 70% at 48 h, whereas at pH 7.4 the release remained below 30%, confirming that the nanocarriers are pH-responsive. This difference is attributed to protonation-induced loosening or swelling of the chitosan layer in acidic environments, facilitating drug diffusion. The pH-dependent release was further confirmed by fluorescence spectroscopy (Figure 3D),

where DOX released at pH 5.5 exhibited significantly stronger fluorescence intensity near 590 nm than that at pH 7.4, consistent with a higher concentration of released DOX under acidic conditions.

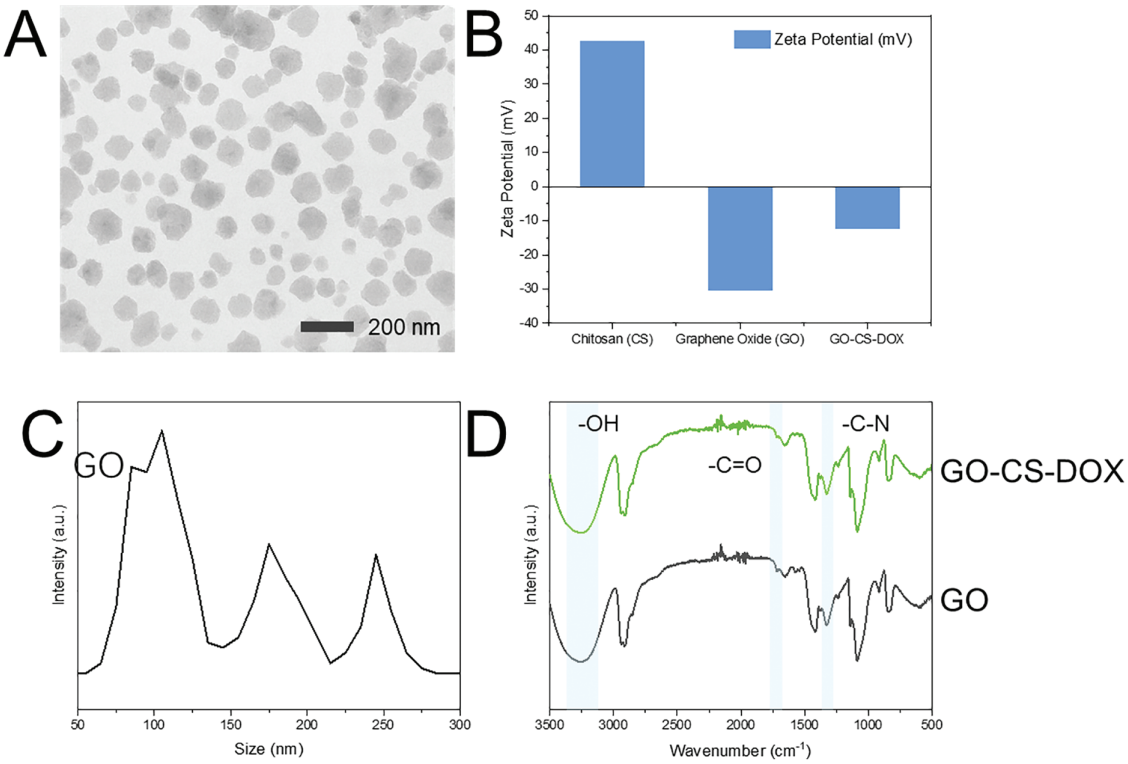

Figure 2. Physicochemical characterization of GO-CS-DOX nanocarriers. (**A**) TEM image showing the morphology and polydisperse size distribution of GO-CS-DOX particles. (**B**) Zeta potential of GO, GO-CS, and GO-CS-DOX, confirming successful surface functionalization. (**C**) DLS size distribution showing increased hydrodynamic diameter after CS coating and DOX loading. (**D**) FTIR spectra of GO (black) and GO-CS-DOX (green). Characteristic peaks of GO at ~3400 cm^{-1} (–OH), ~1720 cm^{-1} (C=O), and ~1620 cm^{-1} (C=C) were observed. After chitosan and DOX modification, the GO-CS-DOX spectrum exhibited additional peaks at ~1560 cm^{-1} (N–H bending), ~1380 cm^{-1} (C–N stretching), and ~1100 cm^{-1} (C–O–C), confirming successful conjugation

In Figure 4, to assess the cytotoxicity and uptake behavior of the DOX-loaded nanocarrier, we first compared the cell viability of gastric cancer cells (MKN-45) after exposure to Free DOX, GO-CS, and GO-CS-DOX at a fixed DOX concentration (5 μg/mL) across 12, 24, and 48 h. As shown in Figure 4A, the GO-CS-DOX group exhibited significantly stronger cytotoxicity than the Free DOX group at each time point, suggesting enhanced therapeutic efficacy. GO-CS alone showed mild toxicity, likely due to partial interactions between GO and the cell membrane. To further explore intracellular uptake, we measured the fluorescence intensity of DOX in cells at each time point (Figure 4B). GO-CS-DOX showed markedly higher cellular uptake than Free DOX at 24 and 48 h, indicating improved delivery efficiency via the nanocarrier. Additionally, a dose-response study was conducted over a wide DOX concentration range (0.1 to 10 μg/mL), and IC50 values were calculated (Figure 4C). GO-CS-DOX showed slightly lower IC50 than Free DOX, confirming its improved potency. Live/dead cell staining (Figure 4D) further validated these findings: GO-CS-DOX treatment resulted in more extensive red fluorescence, consistent with increased cell death.

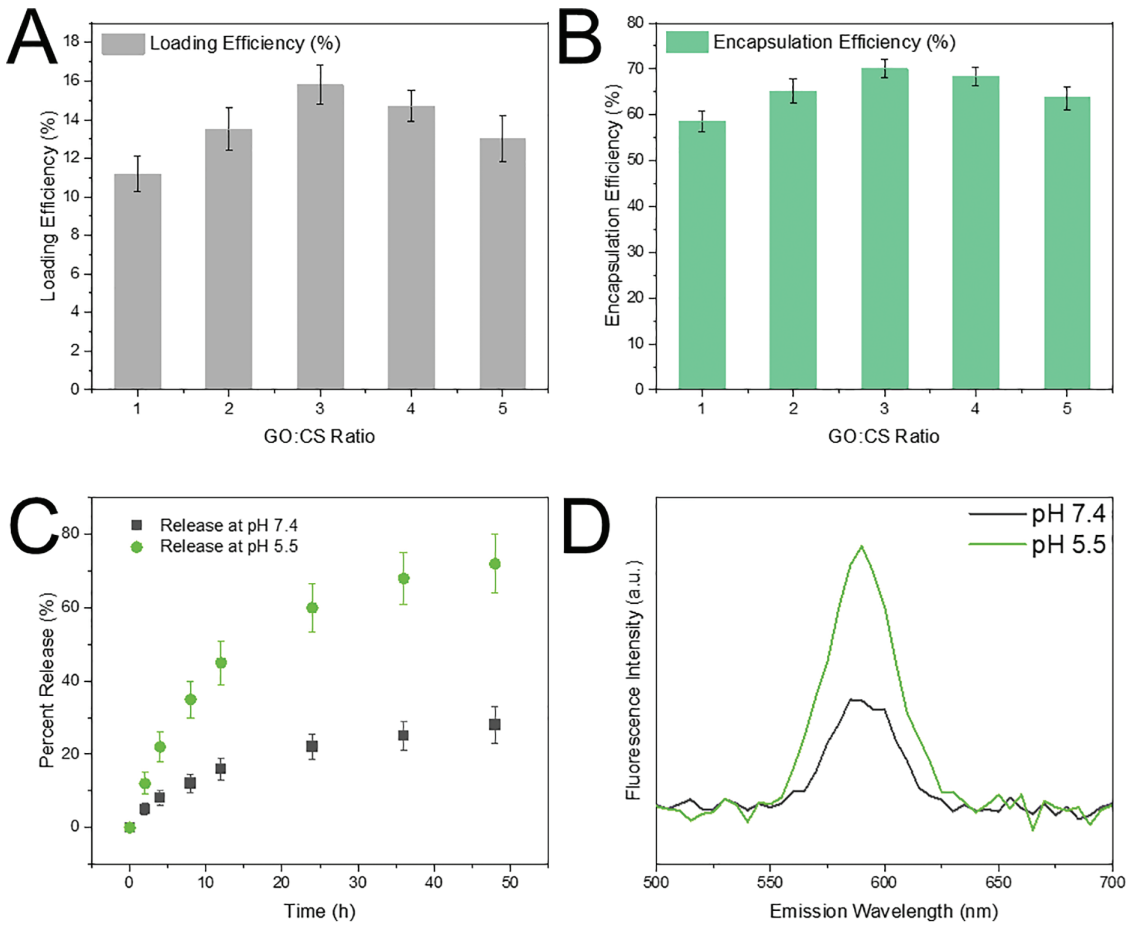

Figure 3. Physicochemical and pH-responsive release characterization of GO-CS-DOX nanocarriers. (**A**) Drug loading efficiency at different GO:CS mass ratios. (**B**) Encapsulation efficiency corresponding to each ratio. (**C**) *In vitro* cumulative release profiles of DOX from GO-CS-DOX under pH 7.4 and pH 5.5 conditions. (**D**) Fluorescence spectra of DOX released at pH 7.4 and pH 5.5, showing emission intensity differences

4. Discussion

Figure 1 demonstrates the fundamental mechanism underlying the intelligent drug release behavior of GO-CS-DOX nanocarriers. The strong pH-responsiveness is attributed to the protonation of amino groups on the chitosan backbone under acidic conditions, which enhances swelling and permeability. This behavior ensures minimal drug leakage in normal tissues while facilitating targeted release at the tumor site. Such a design not only improves drug bioavailability and tumor selectivity but also reduces off-target toxicity [20]. The illustration in Figure 1 clearly conveys the reversible and tunable nature of the system, supporting its application in pH-sensitive chemotherapy for gastric cancer.

Figure 2 provides detailed evidence supporting the successful synthesis and structural integrity of the GO-CS-DOX nanoplatform. The morphology observed in Figure 2A, with irregular yet nanoscale particles, is advantageous for tumor uptake via the enhanced permeability and retention (EPR) effect. The polydispersity also suggests a potentially favorable surface area for drug loading. The surface charge evolution shown in Figure 2B not only confirms each modification step but also reflects changes in colloidal stability. The strong positive charge after CS coating ensures electrostatic interaction with negatively charged cell membranes, while the reduced but still negative surface after DOX loading helps balance circulation stability and uptake efficiency [21]. The DLS data in Figure 2C further supports this surface evolution, as increases in size are directly correlated with the formation of an outer polymeric

and drug layer. This increase in hydrodynamic radius is an indirect but powerful indicator of successful stepwise assembly. Meanwhile, the FTIR spectra in Figure 2D provide chemical-level verification [20]. The observed shifts and emerging peaks associated with amide, hydroxyl, and aromatic groups are strong indicators of molecular interactions among GO, CS, and DOX. Together, the data from Figure 2 confirm not only the structural success of GO-CS-DOX nanocarriers but also their physicochemical suitability for downstream applications, such as pH-triggered drug release and enhanced cellular uptake [22]. This thorough characterization lays a strong foundation for interpreting the subsequent biological performance and therapeutic efficacy of the system [23]. Although the colloidal stability of the GO-CS-DOX formulation was not extensively assessed in serum-containing media in this study, preliminary observations indicate a moderate increase in particle size when dispersed in complete culture medium. This suggests partial aggregation may occur, which is a common phenomenon for nanomaterials in biological fluids due to protein adsorption and ionic strength effects. Despite this, the dispersion remained visually stable over 24 h without visible precipitation. Further investigations, including long-term stability and protein corona analysis, are warranted in future work to fully characterize the biological behavior of the nanocarrier.

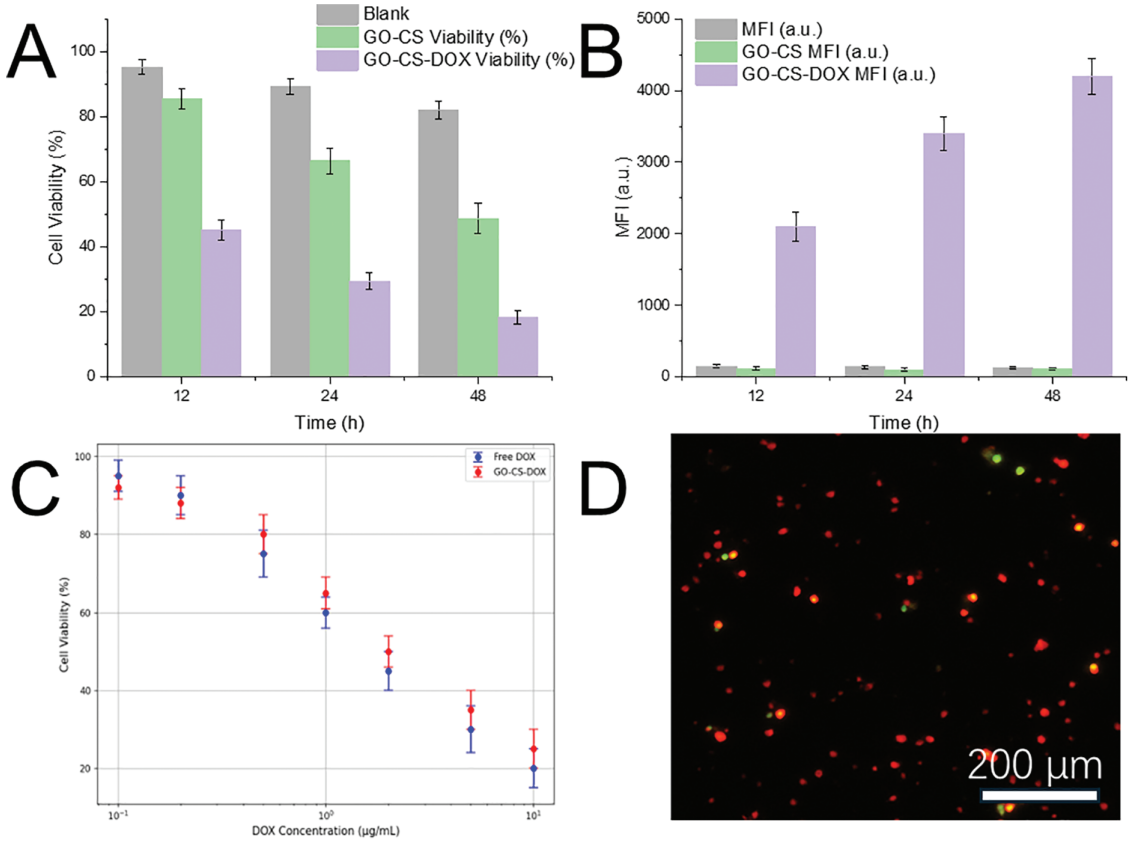

Figure 4. (**A**) Cell viability of gastric cancer cells (MKN-45) after treatment with Free DOX, GO-CS, and GO-CS-DOX at 5 μg/mL DOX equivalent concentration for 12, 24, and 48 h. (**B**) Cellular uptake of DOX from Free DOX and GO-CS-DOX formulations at the same DOX concentration and time points. (**C**) Dose-response curves of Free DOX and GO-CS-DOX at varying concentrations (0.1–10 μg/mL) after 48 h incubation. (**D**) Live/dead cell staining images after GO-CS-DOX 48 h treatment, where live cells appear green and dead cells red. Scale bar: 200 μm

Figure 3 comprehensively illustrates that the GO-CS-DOX nanocarriers possess favorable drug loading properties and strong pH-responsive release behavior. The trends in Figure 3A,B indicate that

drug loading and encapsulation are not linearly dependent on the GO:CS ratio; instead, there exists an optimal formulation (GO:CS = 3:1) where the CS content is sufficient to stabilize the particles and assist in drug binding without overly shielding the GO surface. The data in Figure 3C clearly validate the design of this system as an acid-triggered delivery platform. The release profile demonstrates a fast-sustained release under pH 5.5, consistent with the acidic extracellular environment of solid tumors, particularly gastric cancer [24]. The minimal release at pH 7.4 implies that premature drug leakage can be effectively avoided under normal physiological conditions [25]. Figure 3D provides spectral-level evidence of this differential release, where higher emission intensity at acidic pH confirms the higher release rate of DOX [26,27]. Together, the results in Figure 3 support the functionality of GO-CS-DOX as a responsive, tumor-targeted drug delivery vehicle with high encapsulation capacity and minimal off-target release, thus offering great potential for safe and effective chemotherapy.

The enhanced therapeutic effect of GO-CS-DOX over Free DOX, as demonstrated in Figure 4, can be attributed to the increased cellular uptake and sustained intracellular drug retention enabled by the nanocarrier. GO-CS facilitates DOX transport across the cell membrane and improves drug release under acidic conditions characteristic of tumor microenvironments. This is reflected in the significantly greater uptake (Figure 4B) and cytotoxicity (Figure 4A,C) in the GO-CS-DOX group. The Live/Dead staining image (Figure 4D) provides direct visual evidence of increased cell death, further validating the improved efficacy of the DOX-loaded formulation. Although the GO-CS carrier alone exhibited mild cytotoxicity, this effect was limited and did not interfere with the interpretation of DOX-specific effects. Overall, the results in Figure 4 support the potential of GO-CS as an effective nanocarrier for chemotherapy enhancement in gastric cancer treatment.

5. Conclusion

In this study, we developed a pH-responsive GO-CS-DOX nanocarrier for controlled chemotherapy drug delivery in the acidic tumor microenvironment. The nanoparticles exhibited uniform morphology, moderate loading and encapsulation efficiency, and clear pH-triggered DOX release behavior. *In vitro* fluorescence and release assays confirmed enhanced drug release and fluorescence intensity under acidic conditions (pH 5.5). Preliminary cellular studies suggested increased uptake and reduced viability in gastric cancer cells upon GO-CS-DOX treatment. However, the current results are limited to *in vitro* observations, and no further mechanistic or *in vivo* validation has been performed. Additionally, the cellular data remain insufficient to draw strong conclusions about therapeutic efficacy. Future studies will focus on deeper mechanistic investigations, cellular pathways involved, and *in vivo* evaluation to fully assess the potential of this pH-responsive system in gastric cancer treatment.

Acknowledgement: Not applicable.

Funding Statement: The study was supported by Jiangsu Provincial Research Hospital (YJXYY202204-YSB20) and The Science and Technology Project of Nantong Municipal Health Commission (MS2023016, MS2023109) with Yang Yang.

Author Contributions: All authors contributed to this present work: [Wei Cao] designed the study, [Li Ming] acquired the data, [Qi Shao] interpreted the data. [Jun Zhu] drafted the manuscript, [Yang Yang] and [Weichang Chen] revised the manuscript. All authors reviewed the results and approved the final version of the manuscript.

Availability of Data and Materials: The datasets generated and/or analyzed during the current study are available from the corresponding author Weichang Chen upon reasonable request.

Ethics Approval: Ethics approval was not required for this study because it is not involved any human experiments.

Conflicts of Interest: The authors declare no conflicts of interest to report regarding the present study.

References

1. Dilawar H, Ahmed A, Habib S, Iqbal J, Abdul Rehman T, Hadi I, et al. Gastric metastasis from invasive lobular breast cancer, resembling primary gastric cancer. J Nucl Med Technol. 2024;52(1):68–70. doi:10.2967/jnmt.123.266035.
2. do Carmo GC, Cavalcante RM, de Aquino TMF. Gastric cancer: an overview. Rev Assoc Med Bras. 2024;70(suppl 1):e2024S116. doi:10.1590/1806-9282.2024s116.
3. Alagesan P, Goodwin JC, Garman KS, Epplein M. Cancer progress and priorities: gastric cancer. Cancer Epidemiol Biomark Prev. 2023;32(4):473–86. doi:10.1158/1055-9965.epi-22-0994.
4. Boilève J, Touchefeu Y, Matysiak-Budnik T. Clinical management of gastric cancer treatment regimens. In: Backert S, editor. *Helicobacter pylori* and gastric cancer. Current topics in microbiology and immunology. Berlin/Heidelberg, Germany: Springer; 2023. p. 279–304. doi:10.1007/978-3-031-47331-9_11.
5. Ahmed T, Noman M, Qi Y, White JC, Qi X. Protein nanocarrier-enabled plant genetic engineering systems. Trends Biotechnol. 2025;43(3):498–501. doi:10.1016/j.tibtech.2024.08.009.
6. Chung YK, Hsu CY, Wang YT, Tran TTP, Alalaiwe A, Fang JY. Nanocarrier-enabled delivery of natural antiobesity agents. Nanomedicine. 2025;20(16):2167–87. doi:10.1080/17435889.2025.2534328.
7. Chen J, Lin A, Luo P. Advancing pharmaceutical research: a comprehensive review of cutting-edge tools and technologies. Curr Pharm Anal. 2024;21(1):1–19. doi:10.1016/j.cpan.2024.11.001.
8. Gharatape A, Sadeghi-Abandansari H, Seifalian A, Faridi-Majidi R, Basiri M. Nanocarrier-based gene delivery for immune cell engineering. J Mater Chem B. 2024;12(14):3356–75. doi:10.1039/d3tb02279j.
9. Chakraborti I, Basak U, Roy S, Pakhira M, Das A, Chatterjee DP. Multi-emissive graphene oxide quantum dots with remarkable pH-responsive long-wavelength emission. Nanoscale. 2025;17(21):13387–402. doi:10.1039/d5nr00526d.
10. Han L, Song T, Wang X, Luo Y, Gu C, Li X, et al. miR-21 responsive nanocarrier targeting ovarian cancer cells. Comput Struct Biotechnol J. 2024;24:196–204. doi:10.1016/j.csbj.2024.02.021.
11. Lim DV, Woo WH, Lim JX, Loh XY, Soh HT, Lim SYA, et al. Targeting mutant-p53 for cancer treatment: are we there yet? Curr Mol Pharmacol. 2023;17:e140923221042. doi:10.2174/1874467217666230914090621.
12. Hwang J, Carr J. Lymphadenectomy for gastric cancer. Surg Clin North Am. 2025;105(1):47–54. doi:10.1016/j.suc.2024.06.005.
13. Lee NR, Song EK, Jeon SY. Intramural gastric abscess misdiagnosed as advanced gastric cancer. Arch Iran Med. 2023;26(9):542–6. doi:10.34172/aim.2023.79.
14. Jiang Y, Lei L, Zhao M, Tian Y, Huang Y, Yang M. Nanocarrier vaccines for respiratory infections. Trends Mol Med. 2025;31(7):652–68. doi:10.1016/j.molmed.2024.12.002.
15. Karati D, Kumar D. Molecular insight into the apoptotic mechanism of cancer cells: an explicative review. Curr Mol Pharmacol. 2024;17:e18761429273223. doi:10.2174/0118761429273223231124072223.
16. Lakshmipriya T, Gopinath SCB. Aptamer-decorated nanocarrier for selectively targeting cancer cells. Pharm Nanotechnol. 2025;13(5):839–41. doi:10.2174/0122117385372567250304072634.
17. Mendes-Rocha M, Pereira-Marques J, Ferreira RM, Figueiredo C. Gastric cancer: the microbiome beyond *Helicobacter pylori*. In: Backert S, editor. *Helicobacter pylori* and gastric cancer. Current topics in microbiology and immunology. Berlin/Heidelberg, Germany: Springer; 2023. p. 157–84. doi:10.1007/978-3-031-47331-9_6.
18. Dart A. Intercepting gastric cancer. Nat Rev Cancer. 2024;24(10):651. doi:10.1038/s41568-024-00748-w.

19. Huang S, Huang T, Liu M, Liu D, Hu X, Zhu W, et al. Hyperbranched polymers-functionalized Zein as tumor microenvironment-responsive drug delivery system for sustained and controlled release of doxorubicin. J Drug Deliv Sci Technol. 2025;113:107333. doi:10.1016/j.jddst.2025.107333.
20. Punnoy P, Siripongpreda T, Henry CS, Rodthongkum N, Potiyaraj P. Novel theranostic wounds dressing based on pH responsive alginate hydrogel/graphene oxide/levofloxacin modified silk. Int J Pharm. 2024;661:124406. doi:10.1016/j.ijpharm.2024.124406.
21. Pandey S, Joshi S, Tripathi P, Gupta A, Yadav JS. A review on targeting tunable nanocarrier interaction, physiochemical properties, and futuristic nanocarrier. Biochim Biophys Acta Mol Basis Dis. 2025;1871(7):167956. doi:10.1016/j.bbadis.2025.167956.
22. Sundar R, Nakayama I, Markar SR, Shitara K, van Laarhoven HWM, Janjigian YY, et al. Gastric cancer. Lancet. 2025;405(10494):2087–102. doi:10.1016/S0140-6736(25)00052-2.
23. Shaw S, Pore SK, Liu D, Kumeria T, Nayak R, Bose S. Combating chemoresistance: current approaches & nanocarrier mediated targeted delivery. Biochim Biophys Acta Rev Cancer. 2025;1880(2):189261. doi:10.1016/j.bbcan.2025.189261.
24. Steinauer A. Protein engineering and directed evolution for nanocarrier innovation: medicinal chemistry and chemical biology highlights. CHIMIA. 2024;78(12):885–8. doi:10.2533/chimia.2024.885.
25. Zhang Y, Zhang Y, Ding R, Zhang K, Guo H, Lin Y. Self-assembled nanocarrier delivery systems for bioactive compounds. Small. 2024;20(26):e2310838. doi:10.1002/smll.202310838.
26. Wang Y, Yan H, Ma M, Zhou C, Hou Q, Xu Z, et al. Graft-crosslinked graphene oxide nanofiltration membrane with pH-responsive nanochannels. Polym Adv Technol. 2024;35(1):e6250. doi:10.1002/pat.6250.
27. Zucaro L, Longobardi C, Miele A, Villanova A, Suzumoto Y. Nanocarrier-based drug delivery systems targeting kidney diseases. Kidney Blood Press Res. 2024;49(1):884–97. doi:10.1159/000541848.

Received: 28 August 2025; Accepted: 10 November 2025; Published: 31 March 2026